agronomy

MDPI

Article

Design and Test of Peanut Root-Disk Full-Feeding Longitudinal Axial Flow Pod-Picking Device

Xiaodong Liu, Qingqing Lü, Liquan Yang * and Guangxi Li

Henan Province Engineering Research Center of Ultrasonic Technology Application, Pingdingshan University, Pingdingshan 467000, China; 26131@pdsu.edu.cn (X.L.); 2696@pdsu.edu.cn (Q.L.); 2677@pdsu.edu.cn (G.L.)
* Correspondence: 2695@pdsu.edu.cn

Abstract: To improve the pod-picking efficiency of the combine harvester for both peanut seedlings and peanuts, a longitudinal axial flow pod-picking device is designed in this study. The fixation and adjustment modes of the pod-picking rod were determined. The pod-picking roller's rotational speed, the pod-picking roller's diameter, the pod-picking roller, the pod-picking roller's effective rod-picking length, and the screw-feeding stirrer's critical parameters were determined by theoretical calculation. A combined design of quadratic regression orthogonal rotation was achieved by using Box-Behnken design (BBD) response surface optimization analysis in Design-Expert, with the linear speed of the pod-picking roller, the clearance between the concave screen and the pod-picking roller, and the spacing between the pod-picking rods as the testing factors, and the picking rate and the crushing rate as the indicators. The optimized parameters are as follows: a linear speed of the pod-picking roller of 6.8 m/s, a clearance between the concave screen and the pod-picking roller of 28.5 mm, and a spacing between the pod-picking rods of 18.60 mm. The performances of conventional peanut full-feeding pod-picking devices and the proposed peanut root-disk full-feeding longitudinal axial flow pod-picking device were investigated and compared to clarify the pod-picking performance of the proposed peanut root-disk full-feeding longitudinal axial flow pod-picking device under optimized parameters. The results showed that the picking and crushing rates of the proposed peanut root-disk full-feeding longitudinal axial flow pod-picking device under optimized parameters were 98.93 and 1.62%, respectively, both of which were superior to those of conventional peanut full-feeding pod-picking devices. A pod-picking device matching the combine harvester for peanut seedlings and peanuts was processed under optimized parameters. Field tests revealed that the picking and crushing rates of the proposed harvester were 99.07 and 1.58%, respectively, meeting the industry standards. These findings are instrumental in the further improvement of peanut pod-picking devices.

Keywords: peanut; full feeding; longitudinal axial flow; pod picking

Citation: Liu, X.; Lü, Q.; Yang, L.; Li, G. Design and Test of Peanut Root-Disk Full-Feeding Longitudinal Axial Flow Pod-Picking Device. *Agronomy* **2023**, *13*, 1103. https://doi.org/10.3390/agronomy13041103

Academic Editor: Simon Pearson

Received: 20 March 2023
Revised: 8 April 2023
Accepted: 11 April 2023
Published: 12 April 2023

1. Introduction

Peanut is an essential agricultural product, and planting technology has been gradually improved. However, the peanut pod-picking process is still unsatisfying, and the low separation efficiency in pod-picking is still an essential factor limiting harvesting efficiency [1–3]. Full-feeding pod picking is a primary method used in peanut harvesting. Nevertheless, peanut seedlings account for more than five-sixths of the total volume of a peanut plant. Thus, a poor picking rate and low efficiency may occur in pod picking due to the interference of peanut seedlings. Meanwhile, peanut seedlings will be crushed during the pod-picking process, and the seedling stems, leaves, and pods will be mixed, making it challenging to sort peanuts. The development direction of peanut full-feeding pod-picking devices improves pod-picking efficiency and reduces the crushing rate.

Peanut pod-picking methods can be subdivided into two types: full-feeding pod-picking and half-feeding pod-picking. According to pods' wet and dry conditions, full-feeding pod-picking devices can be divided into full-feeding fresh fruit-picking devices and

full-feeding dried fruit-picking devices. Pod-picking methods can be divided into longitudinal axial flow pod-picking devices and horizontal axis flow pod-picking devices, where longitudinal axial flow pod-picking devices are more widely used in all types of crops [4–9]. Scholars at home and abroad systematic analyses of peanut pod picking and harvesting and a series of supporting technologies have been reported [10–18]. Gao et al. [19] designed a three-ridge-six-row peanut combine harvester pod-picking device, which effectively improved the peanut combine harvesting efficiency. Zheng et al. [20,21] designed a longitudinal axial flow peanut pod-picking system feeding device. A peanut picking combines a harvester feeding conveying device, solving the pod crushing, seedling, and clogging problems. Wu et al. [22] designed a peanut pod-picking device for interplanting patterns in an orchard. Yu et al. [23] designed a tangential flow dual-roller peanut pod-picking device based on two-stage harvesting. Liu et al. [24] investigated the ability to harvest peanut pods, providing a reference for the design of pod-picking devices. Wang et al. [25] performed theoretical analysis and experiments on critical components of peanut pod-picking devices. Yang et al. [26] designed an intelligent peanut pod-picker (4HJZ-6) with a significantly enhanced intelligence level. Zhang et al. [27] designed a half-feeding peanut pod-picker (HSZ-10) for the half-feeding of peanuts. Xu et al. [28] designed a spike-tooth-type longitudinal axial flow peanut pod-picking device, which reduced the pod-picking crushing rate. Yang et al. [29] investigated the relationship between the mechanical properties of peanuts and their harvesting process, which provided theoretical guidance for improving peanut harvesting technology and device development. Zhang et al. [30] investigated the impact friction characteristics of peanut pod picking under different conditions, providing a data reference for developing and designing mechanized peanut production equipment. Xu et al. [31] investigated the mechanized harvesting characteristics of "Huayu 917", which provided a reference for cultivating and screening peanut varieties that are suitable for mechanized harvesting. These studies provided references for improving peanut pod-picking performance, but none significantly improved the pod-picking efficiency.

In this study, to improve the pod-picking efficiency of the pod-picking device of combine harvesters for both peanut seedlings and peanuts, a peanut root disk (a peanut plant with a specific stubble height obtained by cutting off the upper peanut seedlings and keeping only the lower stem and pods) full-feeding longitudinal axial flow pod-picking device was designed. Critical parameters of the pod-picking device were preliminarily determined through theoretical analysis, and the optimized parameters were determined through multifactor multilevel tests. Finally, a pod-picking device compatible with combine harvesters for peanut seedlings and peanuts was produced, and its field tests were conducted.

2. Materials and Methods

2.1. Structure and Working Principles of the Pod-Picking Device

Figure 1 illustrates the proposed peanut root-disk full-feeding longitudinal axial flow pod-picking device. It consists of a feeding inlet, a screw-feeding inlet, a concave screen, a pod-picking roller, a spiral guide plate, an angle adjusting rod, a speed regulator, and a speed regulating motor. A radial slider can adjust the clearance between the pod-picking roller and the concave screen; pod-picking rods are mounted on an axial sliding chute, and an axial slider can adjust the spacing between the pod-picking rods; the rotational speed of the speed regulating motor can be adjusted by the speed regulator, thus achieving the adjustment of the rotational speed of the pod-picking roller.

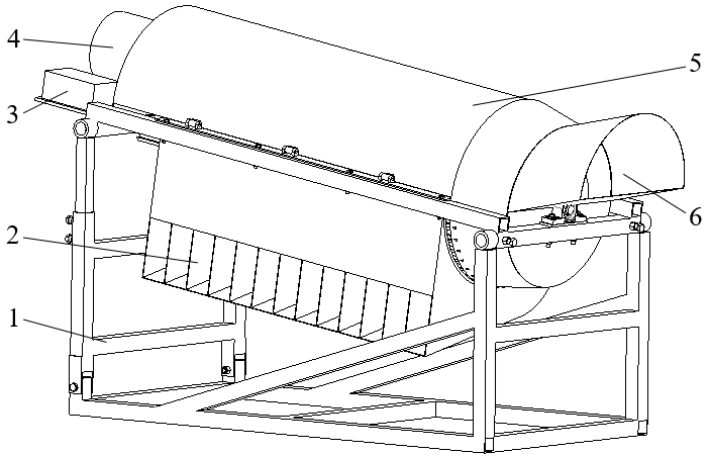

Figure 1. Longitudinal axial flow pod-picking device: 1—angle-adjusting base; 2—feeding outlet; 3—speed regulator; 4—speed regulating motor; 5—pod-picking system; 6—feeding inlet.

During operation, the rotational speed of the speed-regulating motor is adjusted by the speed regulator, and the speed-regulating motor drives the pod-picking roller to rotate. Then, the peanut root disk is subjected to the impact of the grids on the concave screen sieve under the action of the pod-picking roller, thus realizing the separation of peanut seedlings and pods. The separated pods fall into the fruit collection box through the concave screen clearance, and the seedlings move along the axial direction. They are discharged under the action of the axial force of the spiral guide plate. Meanwhile, since the longitudinal axial flow pod-picking device is inclined at a specific degree away from the ground, it can effectively increase the pod-picking distance and improve the picking rate.

2.2. Design of Core Components of the Pod-Picking Device

2.2.1. Fixation and Adjustment of Pod-Picking Rods

Given that a pod-picking device is essential for exploring the optimized pod-picking parameters, its axial, radial, roller rotational speed, and other parameters must be easily adjustable. As core components of the pod-picking device, pod-picking rods shall be uniformly arranged following the spiral lines. This ensures that the pod-picking load of the pod-picking rods is basically the same and also helps the axial movement of the peanut root disk. The pod-picking rods are arranged along single spiral lines (see Figure 2).

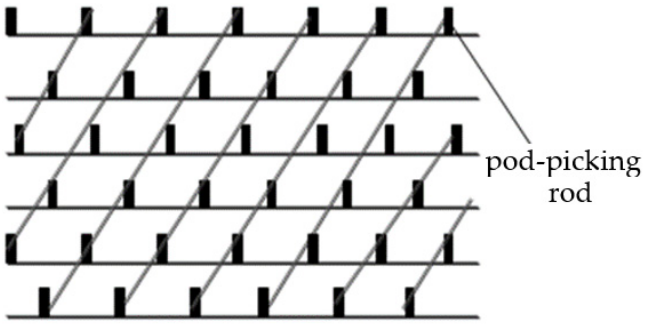

Figure 2. Distribution of the pod-picking rods.

The pod-picking rods are welded on the axial slider, and fastening bolts are installed on the axial slider, which can move in the axial sliding chute and be fixed in the axial sliding chute with fastening bolts. The spacing between the pod-picking rods can be adjusted as needed during the tests. A flange plate is welded on the main shaft of the pod-picking roller, six radial sleeves are welded on both ends of the flange plate, and a radial slider is welded on the bottom of the axial sliding chute. The radial slider works in coordination with the

fastening bolts and the radial sleeves welded on the flange plate, achieving the clearance adjustment between the pod-picking rods and the concave screen. Although the peanut plant is relatively light compared to the whole pod-picking system, a large reaction force is generated when multiple peanut plants are fed into the pod-picking device. Therefore, in the design process, the size of the round steel pod-picking rods should be increased to prevent fatigue deformation of the pod-picking rods under prolonged operation. Based on the size of the pod-picking rods inside the conventional pod-picking device, the pod-picking rods inside the proposed pod-picking device use 12 mm diameter round steel with 45# steel and 60 HRC heat treatment hardness at the working surface. The pod-picking roller is shown in Figure 3.

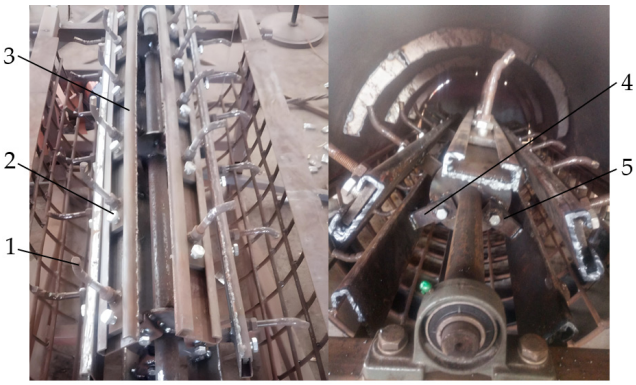

Figure 3. The internal structure of the pod-picking roller: 1—bending tooth; 2—axial slider; 3—axial sliding chute; 4—radial slider; 5—radial sleeve.

2.2.2. Determination of the Rotational Speed of the Pod-Picking Roller

The rotational speed of the pod-picking roller significantly impacts the separation quality of peanut pod-picking. When the rotational speed is relatively high, the pod-picking rods have a high impact on the peanut pods, and the picking rate and crushing rate are high; when the rotational speed is relatively low, the pod-picking rods have a weakening effect on the belt rolling of peanut seedlings, the reaction force of the concave screen decreases, the separation ability of the peanut pods decreases. The picking rate and crushing rate are low. When the rotational speed of the pod-picking roller reaches the critical value, the crushing rate of the peanut pods will increase rapidly, while the power consumption of pod-picking also increases rapidly with increasing rotational speed. An appropriate pod-picking speed is critical to ensuring pod-picking efficiency. Not only should the separation ability of the peanut pods be ensured, but also the crushing rate of the pods should be reduced to reach a balance between the two.

According to the kinetic energy theorem,

$$W = FA = \frac{1}{2}mv^2 \tag{1}$$

$$n = \frac{30v}{\pi r} = 30\sqrt{\frac{2F}{\pi m}} \tag{2}$$

where n is the rotational speed of the pod-picking roller, r/min; v is the linear speed of the roller, m/s; F is the critical pulling force for separation of the peanut pods from the stems, N, 9~12 N; A is the average cross-sectional area of the peanut pods, m^2, equal to 3.14×10^{-4} m^2; and m is the pod-picking roller mass (75 kg, the value obtained by weighing after processing).

The test of peanut seedling and pod separation revealed that the critical force of peanut seedling and pod separation was approximately 10 N. Substituting the known

items into Equations (1) and (2), we obtain the rotational speed of the pod-picking roller of 360–480 r/min.

2.2.3. Determination of the Diameter of the Pod-Picking Roller

The diameter of the pod-picking roller was determined based on the linear speed of the roller and the feeding amount of the peanut root disk. At a constant rotational speed, the linear speed of the roller and the pod-picking ability are positively related to the diameter of the pod-picking roller. However, as the diameter increases, the impact force on the peanut pods increases, which is likely to crush the pods and cause clogging. The forces on the peanut root disk inside the roller were analyzed to determine an appropriate diameter for the pod-picking roller. Figure 4 shows the radial forces acting on the peanut root disk.

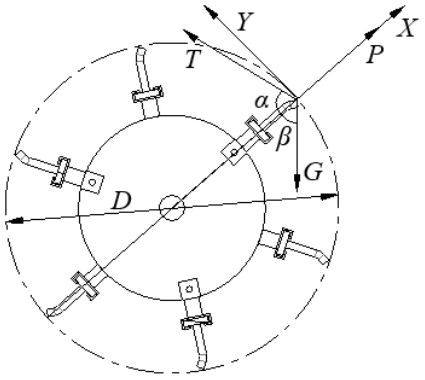

Figure 4. Radial force analysis of the peanut root disk.

According to Figure 4, the force equation of the peanut root disk in the pod-picking device is as follows:

$$P - T\cos\alpha - G\cos\beta > 0 \tag{3}$$

$$P = \frac{m\omega^2 D}{2} > 0 \tag{4}$$

where P is the centrifugal force on the peanut root disk, N; T is the tensile force on the peanut root disk, N; G is the gravity on the peanut root disk, N; α is the radial angle between T and the roller, (°); β is the radial angle between the gravity on the peanut root disk and the roller, (°); m is the mass of the peanut root disk, kg; ω is the angular speed of the roller, rad/s; and D is the roller diameter, mm.

To ensure the smooth discharge of the peanut root disk, we take $\alpha = \beta = 0$ and then obtain the following:

$$D > \frac{2(T+G)}{m\omega^2} \tag{5}$$

Substituting the known data into the formula, it can be determined that the pod-picking roller diameter exceeds 400 mm.

2.2.4. Determination of the Effective Pod-Picking Length of the Pod-Picking Roller

The longer the pod-picking roller, the longer the peanut pod-picking distance, and the higher the picking rate. If the pod-picking roller is too short, peanut pods may be discharged before being removed from the seedlings, resulting in a low picking rate. The appropriate length of the roller can be obtained according to the pod-picking roller's diameter, the roller's linear speed when the peanut pods are separated, the spiral guide plate, and other parameters. The pod-picking separation quality is the best when the pod-picking duration exceeds 1 s. Subjected to the action of the pod-picking rods and the guide plate, the peanut root disk moves spirally in the pod-picking device, radially in a

circular motion and axially in a linear motion along the pod-picking roller. The combined action of the pod-picking roller and the spiral guide plate influences the axial motion speed.

To achieve good pod-picking separation performance, the length of the pod-picking roller must meet the following conditions:

$$l = D_1 \tan 30^\circ + (D_1 - \frac{50}{\tan 30^\circ})D_1(z-1) \quad (6)$$

$$zT_g \geq 1 \quad (7)$$

$$v_c = 2\pi nr \quad (8)$$

$$T_g = \frac{1}{n} \quad (9)$$

where D_1 is the diameter of the top cover, mm, 620 mm; z is the number of spiral baffles; T_g is the rotation cycle of the roller, s; v_c is the tangential speed at the tip of the tooth claws (7 m/s); and r is the radius from the tip of the pod-picking rod tooth to the center of the spindle (280 mm).

According to Equations (6)–(9), the peanut root-disk pod-picking roller length should exceed 1200 mm. To reduce the influence of the test, the effective lengths of the horizontal axis flow and the longitudinal axial flow roller are set to 1400 mm.

2.2.5. Determination of the Screw-Feeding Stirrer Parameters

As a feeding component of the peanut root-disk full-feeding longitudinal axial flow pod-picking device, the screw-feeding stirrer needs to meet the requirements of smooth feeding without blockage, minor impact on peanut pods, and no damage to peanut pods. According to the parameters of the combine harvester for both peanut seedlings and peanuts, to effectively offset the inclination of the feeding inlet to help the feeding from the peanut root disk, the screw-feeding stirrer was designed as a conical shape, with a cone angle of 20°. The structure of the screw-feeding stirrer is shown in Figure 5.

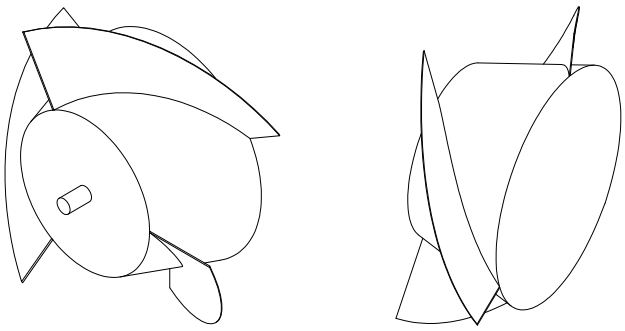

Figure 5. Screw-feeding stirrer.

As a core component of the screw-feeding stirrer, the screw-feeding blade is a crucial factor affecting the feeding performance of the peanut root disk. After the peanut root disk enters the screw-feeding stirrer, it moves toward the pod-picking mechanism at the rear under the action of the screw-feeding blade. The peanut root disk is subjected to axial and radial forces in the screw-feeding stirrer so that the peanut root disk has axial velocity V_1 and circumferential velocity V_2. The velocity analysis diagram is shown in Figure 6.

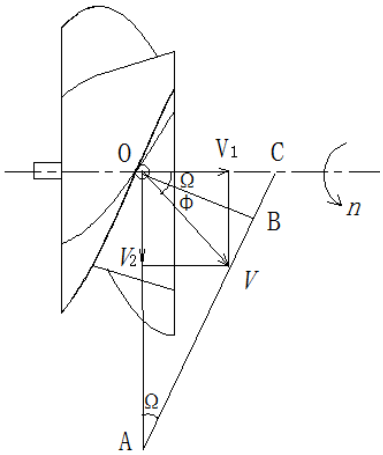

Figure 6. Velocity analysis of the peanut root disk on the screw-feeding blade.

Here $\overline{OA}$ is the circular motion velocity of the peanut root disk. According to the velocity analysis diagram, we obtain

$$V = \overline{OA}\frac{\sin\Omega}{\cos\Phi} = \frac{2\pi Rn}{60}\frac{\sin\Omega}{\cos\Phi} \tag{10}$$

$$\begin{cases} V_1 = V\cos(\Omega+\Phi) = \frac{2\pi Rn}{60}\frac{\cos(\Omega+\Phi)sin\Omega}{\cos\Phi} \\ V_2 = V\sin(\Omega+\Phi) = \frac{2\pi Rn}{60}\frac{\sin(\Omega+\Phi)sin\Omega}{\cos\Phi} \end{cases} \tag{11}$$

where Ω is the screw lift angle (°), Ω = arctan(s/2π*R*); s is the screw pitch, and *R* is the outer circle radius of the screw blade; Φ is the friction angle (°), and μ = tanΦ.

According to the above equations,

$$\begin{cases} V_1 = \frac{sn}{60}\frac{1-\frac{s}{2\pi R}\mu}{(\frac{s}{2\pi R})^2+1} \\ V_2 = \frac{sn}{60}\frac{\frac{s}{2\pi R}\mu}{(\frac{s}{2\pi R})^2+1} \end{cases} \tag{12}$$

According to Equation (12), the motion speed of the peanut root disk is related to the rotational speed of the pod-picking roller n, the screw pitch of the screw-feeding blade s, the friction coefficient between the peanut root disk and the steel plate (3.9~4 in most cases), and the screw-feeding blade radius. According to the previously known conditions, the rotational speed of the pod-picking roller *n* is known, and the radius of the screw blade can be obtained according to the pod-picking roller diameter. To eliminate clogging in the peanut root disk of the pod-picking device, V_1 should be the same as the motion speed of the peanut root disk in the pod-picking device, and V_1 = l/t (t is greater than or equal to 1 s). Substituting the known data into the equation, we obtain $s \leq 800$ mm.

2.3. Experimental Design and Analysis

The peanut pod-picking process is complex, and the pod-picking efficiency is affected by multiple factors. Therefore, the peanut pod-picking device designed through theoretical analysis needs to be tested to verify the device's actual performance. However, tests still have limitations, and conducting a perfect test verification is unrealistic. Given this, this study selected the main factors affecting the pod-picking efficiency, the linear speed of the pod-picking roller, the clearance between the concave screen and the pod-picking roller, and the spacing between pod-picking rods as experimental factors, took the picking rate and the crushing rate as the test indicators, and adopted the Box-Behnken design (BBD) response surface optimization method for quadratic regression orthogonal rotation. In the test, each set of tests was repeated three times, and the average value was obtained to obtain the optimized parameters of the pod-picking device. Meanwhile, pod-picking

tests were conducted based on the optimized parameters further to verify the pod-picking performance of the proposed pod-picking device. A comparison was made between the proposed device and the conventional peanut full-feeding pod-picking device.

The picking rate can be calculated as follows:

$$C_z = \frac{W_z - W_w}{W_z} \times 100\% \tag{13}$$

where C_z is the picking rate (%), W_z is the total mass of the pods (kg), and W_w is the mass of unpicked pods (kg).

The crushing rate can be calculated as follows:

$$C_p = \frac{W_p}{W_z} \times 100\% \tag{14}$$

where C_p is the crushing rate (%), W_z is the total mass of the pods (kg), and W_p is the mass of broken pods (kg).

Figure 7 illustrates the peanut pod-picking device. Where figure a is a peanut root disk full-feeding longitudinal axial flow pod-picking device, figure b is a combine harvester for both peanut seedlings and peanuts. The test material is the peanut root disk with a specific stubble height obtained from the combine harvester for both peanut seedlings and peanuts, as shown in Figure 8.

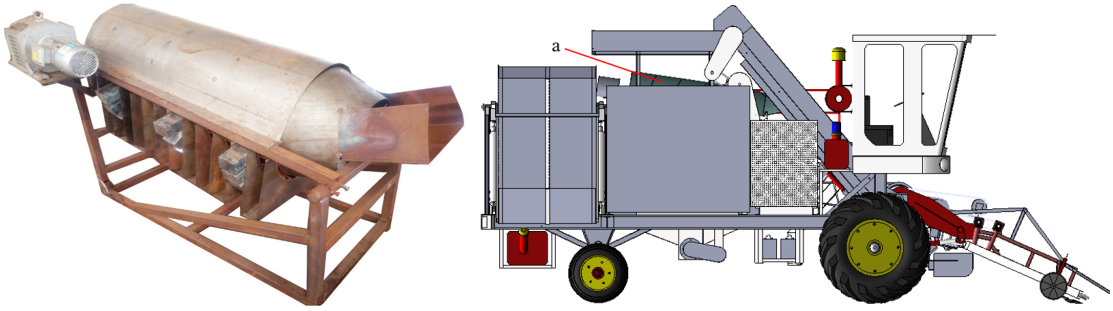

(**a**) (**b**)

Figure 7. Peanut pod-picking device. (**a**) Peanut root disk full-feeding longitudinal axial flow pod-picking device. (**b**) Combine harvester for both peanut seedlings and peanuts (a is the Peanut root disk full-feeding longitudinal axial flow pod-picking device).

(**a**) (**b**)

Figure 8. Acquisition of peanut root disk. (**a**) The front-end double disc cutter of the combine harvester separates the peanut root disk from the peanut plant. (**b**) Peanut root disk.

Fifty peanut root disks were used, and the measured plant parameters were averaged to obtain the parameter values of the peanut root disks, as shown in Table 1. In the test, the pod-picking inclination angle of the longitudinal axial flow pod-picking device was determined to be 20° according to the combined harvester for peanut seedlings and peanuts.

Table 1. Parameters of the peanut root disk.

Stubble Height (mm)	Total Mass of a Single Root Disk (g)	Pod Mass of a Single Root Disk (g)	Stem Dry Moisture Content (%)
63.7	141.33	52.61	38.75

In the test, the rotational speed of the pod-picking separation roller is adjusted by the speed regulating motor in the range of 0~1500 r/min, and the transmission ratio of the speed regulating motor and the pod-picking separation roller is 2:1. Varying types of pod-picking devices on the market result in varying diameters of the pod-picking rollers. Hence, the above speed range of the roller is converted into linear speed for analysis; according to the clearance between the concave screen and the pod-picking roller of the commonly used peanut pod-picking device, the clearance between the concave screen and the pod-picking roller of the proposed device is determined to be in the range of 20~40 mm; the spacing between pod-picking rods takes 200 mm as the middle level and 50 mm as another level. The test factor levels are shown in Table 2.

Table 2. Testing factor levels.

Level	Linear Speed of Pod-Picking Roller V (m/s)	Clearance between the Concave Screen and Pod-Picking Roller G (mm)	Spacing between Pod-Picking Rods S_1 (mm)
+1	9	4	250
0	7	3	200
−1	5	2	150

2.4. Comparative Experiment and Field Test

To verify the pod-picking performance of the proposed peanut root-disk full-feeding longitudinal axial flow pod-picking device under optimized parameters, a comparative experiment was conducted between the conventional peanut full-feeding fresh fruit-picking devices [32] and the proposed peanut root-disk full-feeding longitudinal axial flow pod-picking device by using a small peanut harvester to dig and spread out peanut plants in the field. The proposed peanut root-disk full-feeding longitudinal axial flow pod-picking device conducts the experiment using the processed peanut root disks with a peanut root disk mass of 50 kg and a feeding amount of 1.2 kg/s. In contrast, the conventional peanut full-feeding fresh pod-picking device uses the data listed in an existing paper with the picking and crushing rates as the evaluation indexes.

Meanwhile, to further verify the functional operation performance of the proposed peanut root-disk full-feeding longitudinal axial flow pod-picking device in the field, the longitudinal axial flow pod-picking device compatible with the combine harvester for both peanut seedlings and peanuts was processed and installed on the combine harvester for both peanut seedlings and peanuts to conduct a field test. With the picking and crushing rates as the evaluation indexes and an operating speed of 2.4 km/h, the proposed device had similar effects as the conventional peanut fresh fruit-picking combine harvester, with a continuous traveling distance of 150 m.

3. Results

According to the three-factor, three-level orthogonal rotation combined test, 17 sets of tests were conducted, and the test results are shown in Table 3. Design-Expert software was used for quadratic regression analysis, the regression equations of the picking rate $\boldsymbol{Y}_1$ and the crushing rate $\boldsymbol{Y}_2$ were obtained, and significance tests were conducted.

Table 3. Test scheme and results.

Test No.	Linear Speed of the Pod-Picking Roller X_1	Clearance between the Concave Screen and Pod-Picking Roller X_2	Spacing between Pod-Picking Rods X_3	Picking Rate Y_1 (%)	Crushing Rate Y_2 (%)
1	−1	0	1	98.02	1.15
2	0	0	0	99.38	0.89
3	0	0	0	99.44	0.94
4	1	0	1	97.34	1.53
5	0	1	−1	98.12	0.99
6	1	0	−1	99.26	1.20
7	1	−1	0	99.58	1.61
8	0	0	0	99.21	0.93
9	0	1	1	97.27	1.06
10	−1	0	−1	98.14	0.97
11	0	−1	−1	99.57	1.18
12	0	0	0	99.58	1.02
13	−1	1	0	97.88	0.92
14	1	1	0	98.34	1.21
15	0	−1	1	97.32	1.35
16	−1	−1	0	98.87	1.09
17	0	0	0	99.25	0.93

3.1. Significance Analysis of Picking Rate Y_1

The regression analysis results of the variance of the picking rate $\boldsymbol{Y}_1$ are shown in Table 4. Eliminating the insignificant items, we obtain the quadratic regression model of the picking rate $\boldsymbol{Y}_1$ as follows:

$$\boldsymbol{Y}_1 = 99.37 + 0.20X_1 - 0.47X_2 - 0.64X_3 - 0.46X_1X_3 + 0.35X_2X_3 - 0.29X_1^2 - 0.41X_2^2 - 0.89X_3^2 \quad (15)$$

According to Table 4, the quadratic regression model with $p < 0.01$ is highly significant. The lack-of-fit term with $p > 0.05$ is insignificant, indicating that the fitted model can correctly reflect the relationship between each factor and the error and, thus, reasonably predict the test results. Among the main factors, the spacing between pod-picking rods S_1 significantly affects the picking rate Y_1. Among the interactive factors, the linear speed of the pod-picking roller V and the spacing between pod-picking rods S_1 have the most significant effect on the picking rate Y_1. Here X_2, X_3, X_1X_3, ${X_2}^2$, and ${X_3}^2$ have a highly significant effect, X_1, X_2X_3, and ${X_1}^2$ have a significant effect, and other items have an insignificant effect. According to the regression coefficient of the model, we can rank the items as X_3, X_2, and X_1 according to the effects of the factors on the error in descending order.

Table 4. Regression analysis of variance of Y_1.

Source	Sum of Squares	Degree of Freedom	Mean Square	F-Value	*p*-Value
Model	11.47	9	1.27	24.59	0.0002
X_1	0.32	1	0.32	6.25	0.0410
X_2	1.74	1	1.74	33.56	0.0007
X_3	3.30	1	3.30	63.73	<0.0001
X_1X_2	0.016	1	0.016	0.30	0.6000
X_1X_3	0.81	1	0.81	15.63	0.0055
X_2X_3	0.49	1	0.49	9.46	0.0179
${X_1}^2$	0.36	1	0.36	6.94	0.0337
${X_2}^2$	0.72	1	0.72	13.81	0.0075
${X_3}^2$	3.33	1	3.33	64.32	<0.0001
Residual	0.36	7	0.052		
Lack of fit	0.27	3	0.091	4.10	0.1033
Pure error	0.089	4	0.022		
Cor Total	11.83	16			

Note: $p < 0.01$ indicates a highly significant effect; $0.01 \leq p < 0.05$ indicates a significant effect, and the same is below.

3.2. Significance Analysis of Crushing Rate Y_2

The regression analysis results of the variance of the crushing rate Y_2 are shown in Table 5. Eliminating the insignificant items, we obtain the quadratic regression model of the crushing rate Y_2 as follows:

$$Y_2 = 0.94 + 0.18X_1 - 0.13X_2 + 0.094X_3 + 0.17X_1^2 + 0.099X_2^2 + 0.10X_3^2 \quad (16)$$

Table 5. Regression analysis of variance of Y_2.

Source	Sum of Squares	Degree of Freedom	Mean Square	F-Value	*p*-Value
Model	0.71	9	0.079	22.72	0.0002
X_1	0.25	1	0.25	72.89	<0.0001
X_2	0.14	1	0.14	39.85	0.0004
X_3	0.070	1	0.070	20.33	0.0028
X_1X_2	0.013	1	0.013	3.82	0.0914
X_1X_3	0.0056	1	0.0056	1.63	0.2428
X_2X_3	0.0025	1	0.0025	0.72	0.4233
${X_1}^2$	0.12	1	0.12	33.76	0.0007
${X_2}^2$	0.041	1	0.041	11.93	0.0106
${X_3}^2$	0.046	1	0.046	13.17	0.0084
Residual	0.024	7	0.0035		
Lack of fit	0.015	3	0.005	2.22	0.2281
Pure error	0.0091	4	0.0023		
Cor Total	0.73	16			

According to Table 5, the quadratic regression model with $p < 0.01$ is highly significant. The lack-of-fit term with $p > 0.05$ is insignificant, indicating that the fitted model can correctly reflect the relationship between each factor and the error and, thus, reasonably predict the test results. Here X_1, X_2, X_3, ${X_1}^2$, and ${X_3}^2$ have a highly significant effect, ${X_2}^2$ has a significant effect, and other items have an insignificant effect. According to the regression coefficient of the model, we can rank the items as X_1, X_2, and X_3 according to the effects of the factors on the error in descending order.

3.3. Analysis of Response Surfaces

The test data are processed using Design-Expert. By fixing any factor at the zero level, we obtain the dual-factor response surfaces of the pod-picking performance indicators, as shown in Figure 9.

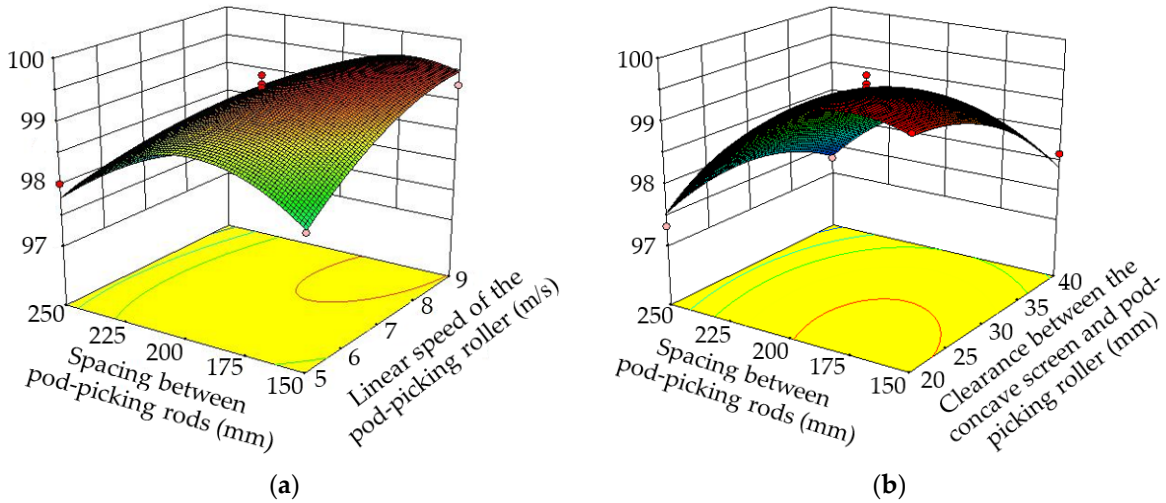

Figure 9. Dual-factor response surfaces of pod-picking performance indicators. (**a**) Y_1, G = 3 mm. (**b**) Y_1, V = 7 m/s.

Figure 9a is the dual-factor response surface of the linear speed of pod-picking roller V and the spacing between pod-picking rods S_1 obtained by fixing the clearance G between the concave screen and the pod-picking roller at the zero level. Figure 9b depicts the dual-factor response surface of the clearance G between the concave screen and the pod-picking roller and the spacing between pod-picking rods S_1 obtained by fixing the linear speed of pod-picking roller V at the zero level. Using the numerical optimization module in Design-Expert, we obtain the optimized parameters as follows: the linear speed of the pod-picking roller is 6.8 m/s, the clearance between the concave screen and the pod-picking roller is 28.5 mm, and the spacing between pod-picking rods is 18.6 mm.

3.4. Results of Comparative Experiment and Field Test

Although the peanut full-feeding pod-picking method is the conventional pod-picking separation method, various issues remain to be solved in this method. By comparing the test results of the conventional peanut full-feeding pod-picking device and the proposed peanut root-disk full-feeding pod-picking device, we can clearly see the advantages and disadvantages of the two methods. By adopting the optimized parameters in the proposed peanut root-disk full-feeding longitudinal axial flow pod-picking device, we obtain picking and crushing rates of 98.93 and 1.62%, respectively, under the optimized parameters. By comparing with the experimental data in studies on the development and experimental study of a full-feeding fresh peanut pod-picking device, we found that regardless of the picking rate or the crushing rate, the proposed peanut root-disk full-feeding longitudinal axial flow pod-picking device shows improved performance compared with the conventional full-feeding fresh peanut pod-picking device. Peanut root-disk feeding separates peanut

seedlings from peanut plants before feeding the plants into the pod-picking device. Compared with the conventional full-feeding fresh peanut pod-picking device, the proposed device has a pod quality in peanut root disks significantly higher than the pod quality in whole peanut plants under the same feeding amount. According to the statistics of the pod quality of the peanut root disks and whole peanut plants, the peanut pod feeding amount of the proposed peanut root-disk pod-picking device can be 2.42 times higher than that of the conventional full-feeding fresh peanut pod-picking device, thus significantly improving the pod-picking efficiency. The full feeding of peanut root disks not only eliminates the impact of peanut seedlings on the pod-picking efficiency but also avoids the clogging of the full-feeding fresh peanut pod-picking device due to a high feeding amount.

The field test is shown in Figure 10. The field test revealed that the proposed combine harvester for peanut seedlings and peanuts could harvest three ridges and six rows of peanuts simultaneously. Thus, its harvesting efficiency is significantly higher than that of the conventional peanut combine harvester. Meanwhile, with the use of the peanut root-disk pod-picking method, almost no unpicked peanut root disks can be seen after pod-picking operations in the field. According to the statistics, the picking and crushing rates are 99.07 and 1.58%, respectively. The proposed device performs better in the field than the conventional pod-picking device. This is because the resonance and the unstable ground affect the movement of the peanut root disks in the pod-picking device when the proposed combine harvester operates in the field, resulting in changes in the pod-picking distance and loading of the peanut root disks in the pod-picking device. This suggests that the proposed peanut root-disk pod-picking device has a positive effect on improving pod-picking efficiency.

(**a**) (**b**)

Figure 10. Field test. (**a**) Field test scene. (**b**) Peanut root-disk after pod-picking.

4. Conclusions

This study proposed a novel method that can effectively improve peanut pod-picking efficiency. A compatible peanut pod-picking device was designed, and which parameters device were optimized through tests, and a comparative experiment and a field test were executed.

(1) The fixation and adjustment methods of pod-picking rods were determined through analysis. The rotational speed of the pod-picking roller (360–480 r/min), the diameter of the pod-picking roller (>400 mm), the effective pod-picking length of the pod-picking roller (1400 mm), and the critical parameters of the screw-feeding stirrer were determined through theoretical calculations. Through multifactor and multilevel tests and Design-Expert, we obtained the optimized parameters as the linear speed of the pod-picking roller of 6.8 m/s, the clearance between the concave screen and the pod-picking roller of 28.5 mm, and the spacing between the pod-picking rods of 18.60 mm.

(2) To further verify the pod-picking performance of the peanut root-disk full-feeding longitudinal axial flow pod-picking device, a comparative experiment and field test were conducted. The comparative experiment revealed that the proposed peanut root-disk full-feeding longitudinal axial flow pod-picking device had pick and crushing rates of 98.93% and 1.62%, respectively, under optimized parameters. The field test revealed that the picking and crushing rates were 99.07% and 1.58%, respectively, both meeting the industry standards and outperforming conventional pod-picking devices.

The study lasted more than a year. This study effectively improved peanut pod-picking efficiency and introduced a novel pod-picking method based on peanut root disks, providing a new idea for efficient peanut pod picking.

Author Contributions: Conceptualization, X.L.; methodology, X.L.; software, X.L.; validation, X.L.; formal analysis, X.L.; data curation, X.L. writing—original draft preparation, X.L.; writing—review and editing, L.Y.; visualization, L.Y.; supervision, Q.L.; project administration, G.L. All authors have read and agreed to the published version of the manuscript.

Funding: This research was funded by the following fund projects: the Key Scientific Research Projects of Henan Province colleges and universities (20A210029); Mechanical Manufacturing and its Automation Key Disciplines of Pingdingshan University (PXY-JXZDXK-202306); Doctoral Scientific Research Foundation of Pingdingshan University (PXY-BSQD-2023023).

Institutional Review Board Statement: Not applicable.

Informed Consent Statement: Not applicable.

Data Availability Statement: Not applicable.

Conflicts of Interest: The authors declare no conflict of interest.

References

1. Yu, J.D.; Liu, Y.F.; Wang, D.W. Design and experimental study of movable peanut picker. *J. Agric. Mech. Res.* **2021**, *43*, 59–65.
2. Wu, T.L. Design and Test of Hanging Small Peanut Picker. Master's Thesis, Xinjiang Agricultural University, Wulumuqi, China, 2022.
3. Fang, Q.L. Innovative Design and Performance Analysis on the Picking Device for Peanut Combine Harvester. Master's Thesis, Hebei Normal University of Science & Technology, Qinhuangdao, China, 2021.
4. Yang, L.Q.; Wang, W.Z.; Zhang, H.M.; Li, L.H.; Wang, M.; Hou, M.T. Improved design and bench test based on tangential flow-transverse axial flow threshing system. *Trans. Chin. Soc. Agric. Eng.* **2018**, *34*, 35–43.
5. Wang, S.Z.; Lu, B.C.; Cao, J.R.; Shen, M.W.; Zhou, C.Q.; Feng, Y. Research on a method for diagnosing clogging faults and longitudinal axial flow in the threshing cylinders of drum harvesters. *Noise Control. Eng. J.* **2021**, *69*, 209. [CrossRef]
6. Tang, Z.; Li, Y.M.; Xu, L.Z.; Kumi, F. Modeling and design of a combined transverse and axial flow threshing unit for rice harvesters. *Span. J. Agric. Res.* **2014**, *12*, 973–983. [CrossRef]
7. Fu, J.; Xie, G.; Ji, C.; Wang, W.; Zhou, Y.; Zhang, G.; Zha, X.; Abdeen, M.A. Study on the distribution pattern of threshed mixture by drum-shape bar-tooth longitudinal axial flow threshing and separating device. *Agriculture* **2021**, *11*, 756. [CrossRef]
8. Wang, R.X.; Zhao, X.P.; Ji, J.T.; Jin, X.; Li, B. Design and performance analysis of tangential-axial flow threshing device for oat harvester. *Int. J. Agric. Biol. Eng.* **2021**, *6*, 61–67. [CrossRef]
9. Petre, I.M. Modeling and simulation of grain threshing and separation in axial threshing units. Part II. Application to tangential feeding. *Comput. Electron. Agric.* **2008**, *60*, 105–109.
10. Wang, B.K.; Gu, F.W.; Cao, M.Z.; Xie, H.X.; Wu, F.; Peng, B.L.; Hu, Z.C. Analysis and evaluation of the influence of different drum forms of peanut harvester on pod-pickup quality. *Agriculture* **2022**, *12*, 769. [CrossRef]
11. Negrete, J.C. Current status and strategies for harvest mechanization of peanut in Mexico. *Int. J. Agric. Environ. Sci.* **2015**, *2*, 7–15.
12. Gao, L.X.; Su, Z.; Chen, Z.Y.; Liu, Z.X.; Lü, C.Y.; Li, H. Design and experiment of double-roller semi-feeding peanut picking device for breeding in mini type area. *Trans. Chin. Soc. Agric. Mach.* **2016**, *47*, 93–98.
13. Wang, S.Y.; Hu, Z.C.; Xu, H.B.; Cao, M.Z.; Yu, Z.Y.; Peng, B.L. Design and test of pickup and conveyor device for full-feeding peanut pickup harvester. *Trans. CSAE* **2019**, *35*, 20–28.
14. Chen, Z.Y.; Guan, M.; Gao, L.X.; Chen, L.J.; Ma, F.; Dong, H.S. Design and test on axial flow peanut picking device with screw bending-tooth. *Trans. Chin. Soc. Agric. Mach.* **2016**, *47*, 106–113.
15. Shi, L.L.; Wang, B.; Hu, Z.C.; Yang, H.G. Mechanism and experiment of full-feeding tangential-flow picking for peanut harvesting. *Agriculture* **2022**, *12*, 1448. [CrossRef]
16. Wang, B.K.; Hu, Z.C.; Cao, M.Z.; Zhang, P.; Yu, Z.Y.; Zhang, C. Design and test of axial-flow peanut picking and harvesting machine. *Trans. Chin. Soc. Agric. Mach.* **2021**, *52*, 109–118.

17. Wang, B.K.; Gu, F.W.; Yu, Z.Y.; Cao, M.Z.; Wang, J.T.; Hu, Z.C. Design and experiment of picking-up mechanism of axial-flow full-feed peanut harvester. *Trans. Chin. Soc. Agric. Mach.* **2020**, *51*, 132–141.
18. Wang, Q.H.; Yu, Z.Y.; Zhang, Y.H.; Li, J.H.; Peng, B.L.; Wang, B.; Hu, Z.C. Experimental study of a 4HLB-4 half-feed four-row peanut combine harvester. *Agronomy* **2022**, *12*, 3094. [CrossRef]
19. Gao, Z.H.; Shang, S.Q.; Wang, D.W.; He, X.N.; Xu, N.; Zheng, J.M.; Zhou, Z.H.; Liu, B. Design and test of three ridge six row peanut combine harvester picking device. *J. Agric. Mech. Res.* **2023**, *45*, 176–181.
20. Zheng, J.M.; Shang, S.Q.; Wang, D.W.; He, X.N.; Zhao, Z.; Zheng, X.S.; Guo, P.; Xu, J.M. Design and test analysis of helical vane of peanut stripper with longitudinal axial flow. *J. Agric. Mech. Res.* **2023**, *45*, 183–189.
21. Zheng, J.M.; Wang, D.W.; Shang, S.Q.; He, X.N.; Xu, N.; Gao, Z.H.; Guo, P.; Zhao, Z.L. Design and experiment of feeding and conveying device for peanut picking combine. *J. Agric. Mech. Res.* **2023**, *45*, 81–87.
22. Wu, T.L.; Guo, H.; Yu, X.D.; Peng, B.; Liu, H.S.; Ye, X.W. Design and experiment of peanut-picking device under interplanting pattern in orchard. *Agric. Res. Arid. Areas* **2021**, *39*, 224–229.
23. Yu, X.D.; Guo, H.; Guo, W.H.; Xue, S.M.; Liu, H.S.; Ye, X.W. Design and motion simulation of pneumatic device for picking up ground jujube. *J. Agric. Mech. Res.* **2021**, *43*, 83–87.
24. Liu, L.; Liu, D.Q.; Sun, Q.T.; Qian, K.; Li, X.J. Experiment and analysis of the harvest and picking ability of peanut. *J. Agric. Mech. Res.* **2022**, *44*, 139–144.
25. Wang, M.; Yang, R.B.; Shang, S.Q.; Wang, F.J.; Wang, Z.Z. Design analysis and test of key equipment for fully fed peanut picking machine. *J. Agric. Mech. Res.* **2021**, *43*, 141–145.
26. Yang, F.J.; Li, H.Q.; Li, Z.P.; Liu, Z.G.; Sun, Y.; Zhang, S.H.; Ma, C.Y. Design and research of 4HJZ-6 intelligent peanut picker. *Agric. Equip. Veh. Eng.* **2020**, *58*, 6–9.
27. Zhang, J.F.; Wang, Z.G.; Jiang, L.M.; Chen, Y.L.; Yan, S.K.; Liu, C.P.; He, Z.P.; Zhou, J. Design and test of HSZ-10 half feed peanut picking machine. *Jiangxi Sci.* **2019**, *37*, 98–102.
28. Xu, N.; Shang, S.Q.; Wang, D.W.; He, X.N.; Gao, Z.; Liu, J.Q.; Zhang, Y.D.; Guo, P. Design and research of spike tooth type peanut picking device with longitudinal. *J. Agric. Mech. Res.* **2020**, *42*, 197–201.
29. Yang, H.G.; Cao, M.Z.; Wang, B.; Hu, Z.C.; Xu, H.B.; Wang, S.Y.; Yu, Z.Y. Design and test of a tangential-axial flow picking device for peanut combine harvesting. *Agriculture* **2022**, *12*, 179. [CrossRef]
30. Zhang, P.; Xu, H.B.; Zhuo, X.R.; Hu, Z.C.; Lian, C.L.; Wang, B. Biotribological characteristic of peanut harvesting impact-friction contact under different conditions. *Agronomy* **2022**, *12*, 1256. [CrossRef]
31. Xu, J.; Chen, M.N.; Chen, N.; Pan, L.J.; Wang, T.; Chen, Y.Z.; Hu, Z.C.; Zou, Z.F.; Yu, S.L.; Cui, F.G.; et al. Experimental study on peanut mechanized harvesting of huayu917. *J. Peanut Sci.* **2021**, *50*, 51–56.
32. Qiu, L.J. Design Full-Feeding Method of High-Moisture Peanut Stripping Equipment and Experimental Analysis. Master's Thesis, Jiangsu University, Zhenjiang, China, 2014.